5.3 Frequency contents

In the following analysis, the exemplary spectral contents are plotted for the three channels for a low speed and high speed with the same, medium torque value.

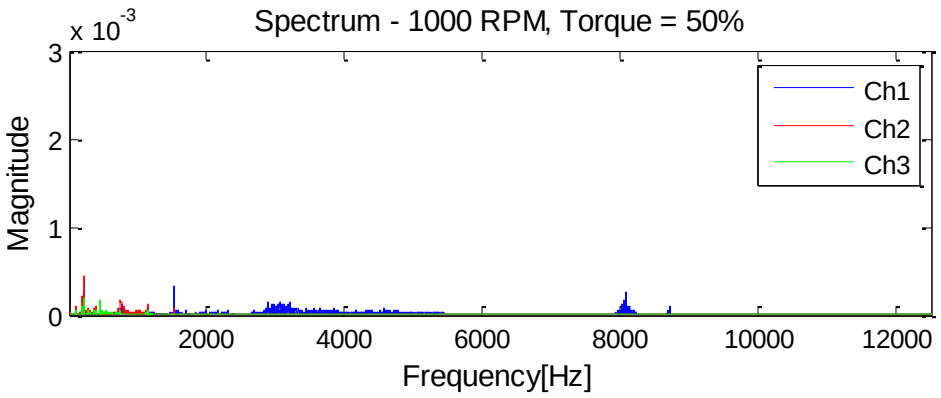

Figure 15. Spectral contents for low speed and medium torque, 3 channels

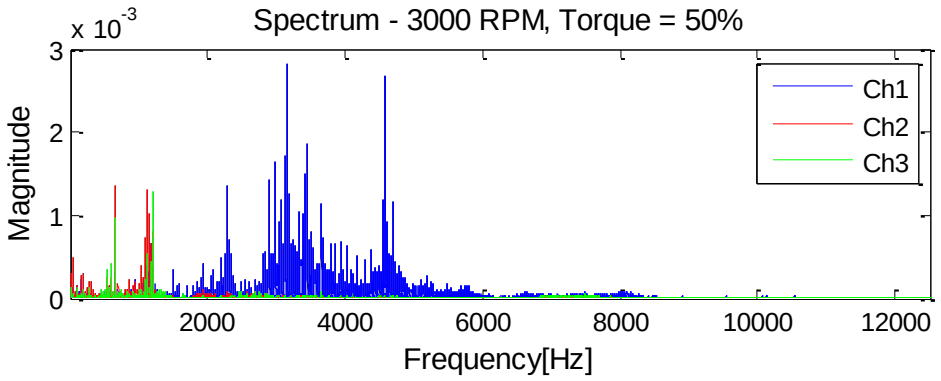

Figure 16. Spectral contents for low speed and medium torque, 3 channels

As observed in figures 15 and 16, the resonant frequencies of the machine are highly induced by higher speed, which shell transform into higher characteristic features values upon upcoming tests. Two resonant frequencies might be identified at this stage, between 3kHz-5kHz, and 8 kHz. Both frequency ranges are covered by sensors' dynamic range.

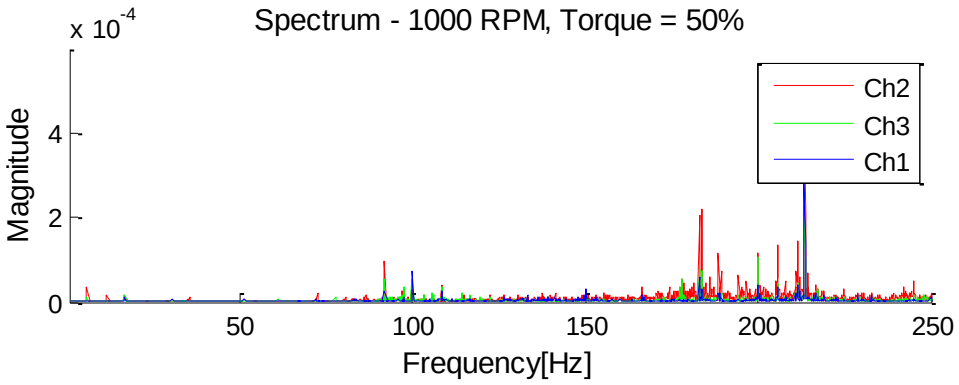

Figure 17. Spectral contents for low speed and medium torque (ZOOM 0Hz -250 Hz)

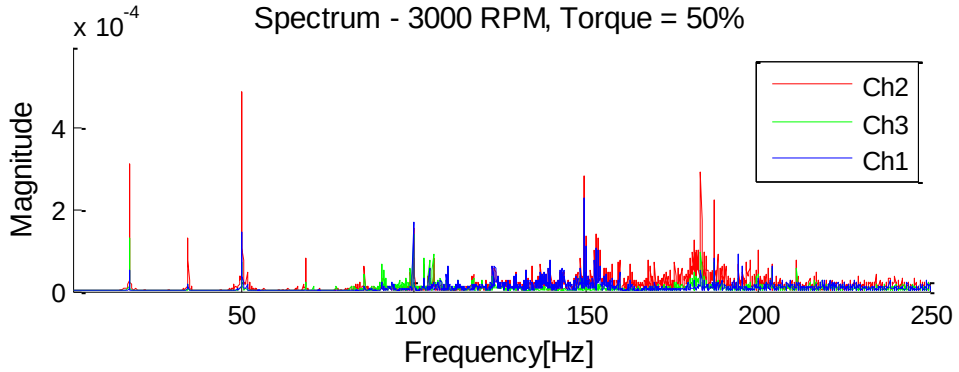

Figure 18. Spectral contents for low speed and medium torque (ZOOM 0Hz -250 Hz)

Figures 17 and 18 illustrate the frequency contents for low frequency range. As illustrated, the dominating components is correlated with the fundamental shaft component. For speed equal 3000 rpm, it is 3000/60 = 50 Hz, and harmonics, i.e. 100 Hz, 150 Hz, 200 Hz. The spectra also contain the 17.1 Hz component, which comes from 49.9/17.1 = 2.9181, which corresponds to the gearbox ratio, as illustrated in figure 19.

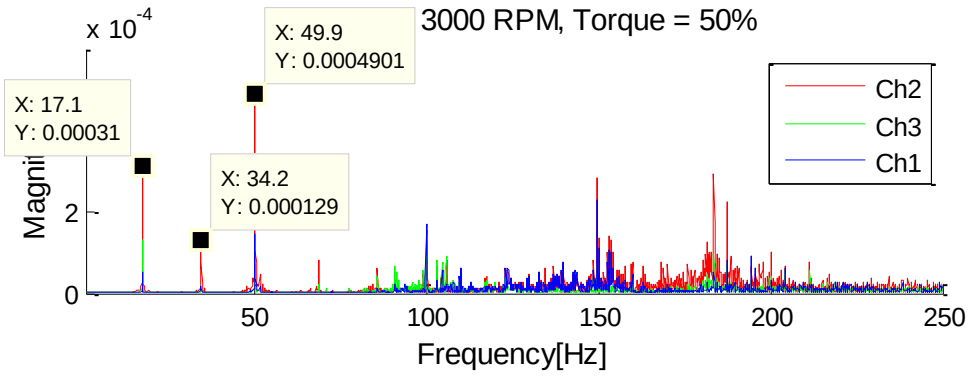

Figure 19. Spectral contents for low speed and medium torque (ZOOM 0Hz -250 Hz) with marked slow shaft harmonics

5.4 Time-frequency characteristics

The time-frequency analysis enables verification of the signal frequency contents as a function of a limited time window. Following figures 20-22 show the result of application of the STFT on each channel for exemplary data.

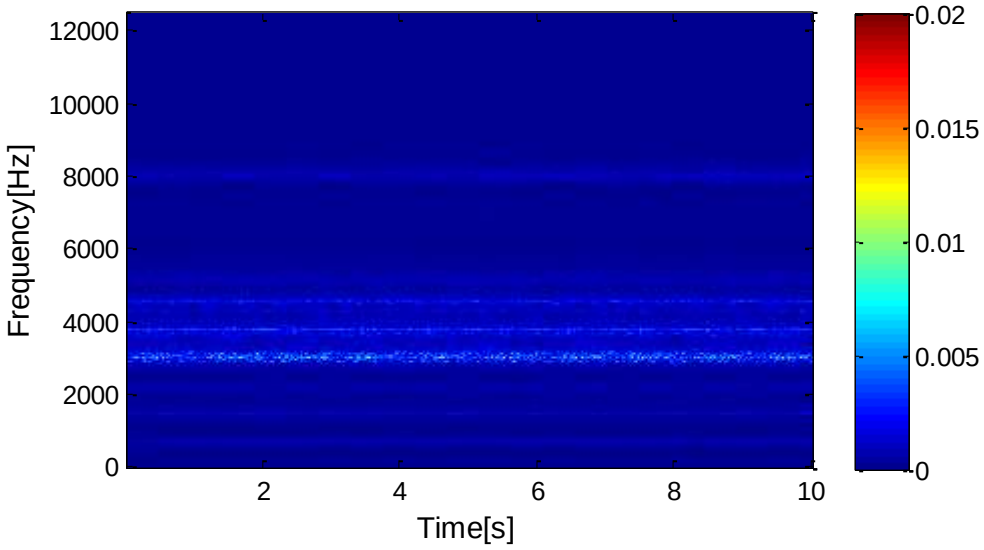

Figure 20. Spectrogram for time signal from channel 1

As observen on the gearbox sensor, the GMF frequencies are constant with time. The machine shows strong resonant freqeuncies around 3kHz and kHz.

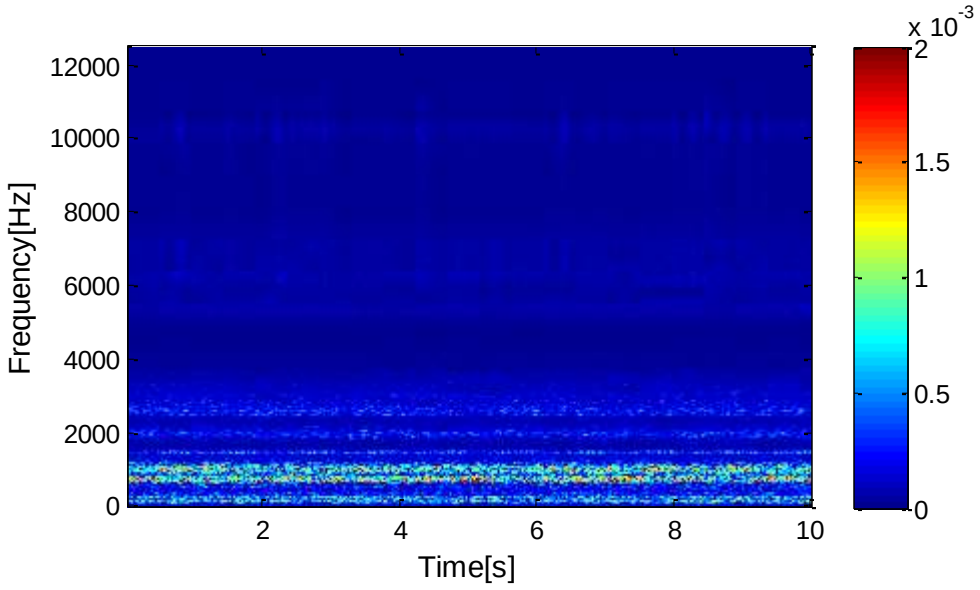

Figure 21. Spectrogram for time signal from channel 2

As observen on the middle bearing sensor, the bearing mounting is susceptible to shaft movement, which manifests in a number of vertical lines in the 6000-12000 Hz range. This phenomenon will be the object of study in subsequent tasks.

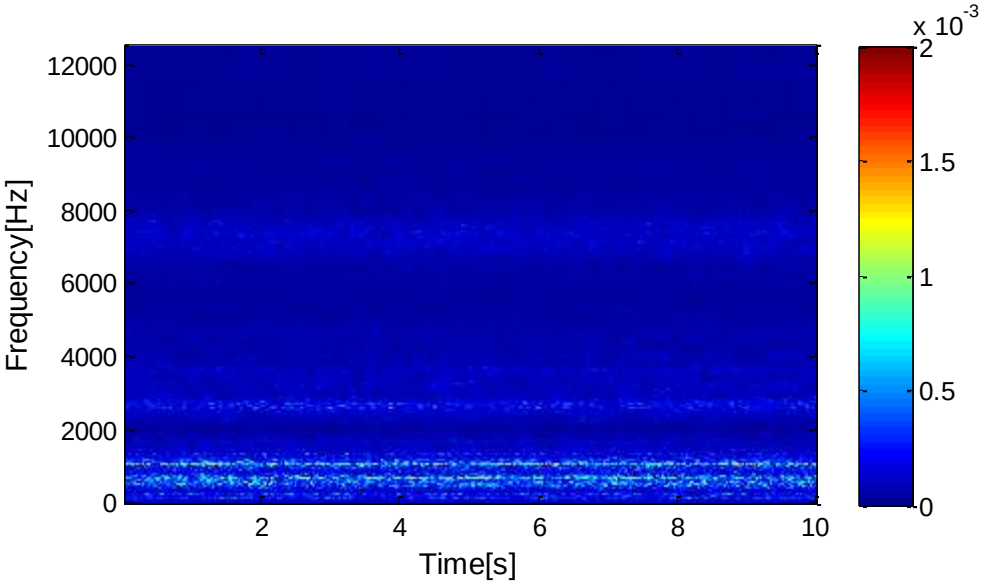

Figure 22. Spectrogram for time signal from channel 3

The channel 3 sensor is correlated with a rigid bearing body, so its readings are very similar to the

readings of sensor 3.

5.5 Preliminary analysis of the wideband diagnostic indicators

For visualization of the outcome of the measurements, Root-Mean-Square (RMS) values of acquired signal as a function of operational conditions (rotational speed and torque) have been plotted. Following figures were obtained by averaging of calculated RMS values from subsequent sessions. Averaging was applied in order to minimize the influence of randomness on the measurement process.

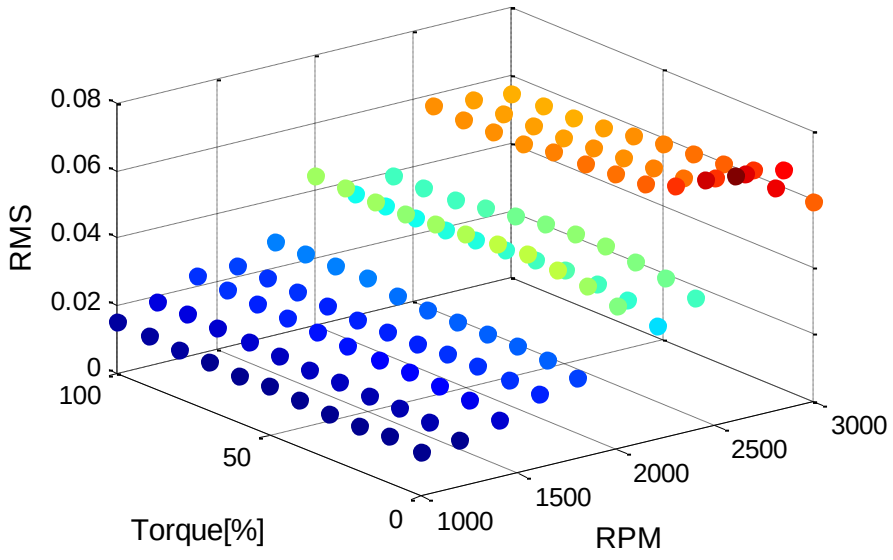

Figure 23. RMS values for each set of operational conditions calculated for signals from channel 1.

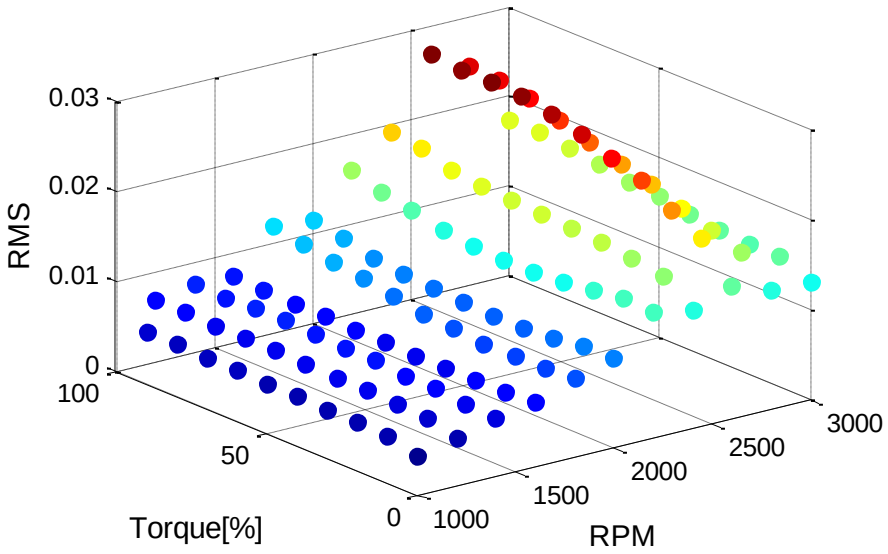

Figure 24. RMS values for each set of operational conditions calculated for signals from channel 2.

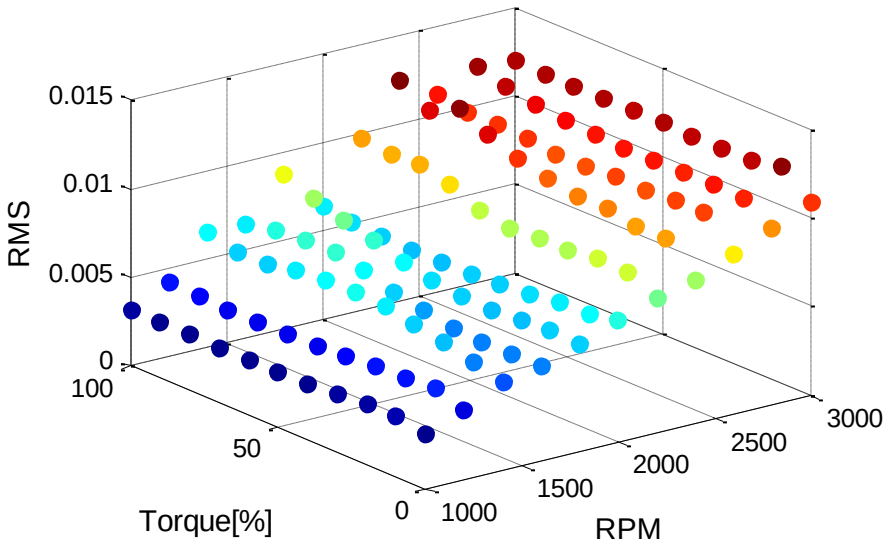

Figure 25. RMS values for each set of operational conditions calculated for signals from channel 3.

For all of measurement channels clear correlation between RMS values and rotational speed can be noticed. Such outcome was expected based on our previous experiences as well as the literature search. However, there were no clear relation between load (here given as a torque [%]) and values of investigated signal RMS. Based on previous preliminary research [ref. 3, 4] as well as literature search

[ref. 1, 2] significant relation between load and vibration based features should be expected. Example of RPM/Load/Vibration-feature dependence for real mechanical system is presented in the figure 26.

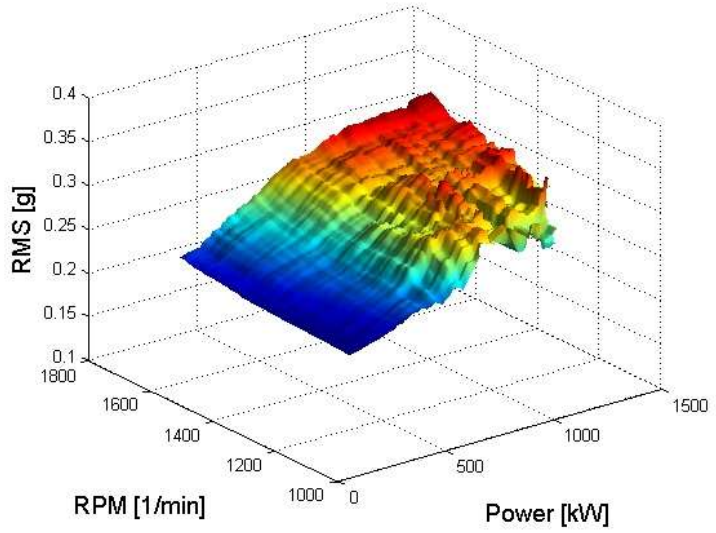

Figure 26. RPM/Load/RMS representation for the wind turbine operating under varying load and speed regime [3]

In order to present scattered RMS data as a three- dimensional surface that could be clear to analyze the authors wish to propose the method that bases on calculation of arithmetic mean of the data in the segments corresponding to chosen ranges of both rotational speed and generator output power. Mean value of RMS calculated for chosen segment is given by:

$$RMS_{\Delta RPM}^{\Delta P}(P, RPM) = \frac{1}{n}\sum_{n=1}^{n} RMS_{RPM'}^{P'}(n), \tag{1}$$

$$P' \subset \left\{P - {}^{\Delta P}/_{2}, P + {}^{\Delta P}/_{2}\right\}, \tag{2}$$

$$RPM' \subset \left\{RPM - {}^{\Delta RPM}/_{2}, RPM + {}^{\Delta RPM}/_{2}\right\}. \tag{3}$$

where P stands for Power. ΔP and ΔRPM are range-widths power and rotational speed respectively

$RMS^{P'}_{RPM'}(n)$ is the nth RMS sample corresponding to the range of power P' and the range of rotational speed RMS'. For presented study ΔP was equal to 200 kW while ΔRPM was equal to 100 RPM [3].

As shown in figure 23 on the example of wind turbine, for real-life mechanical object dependence between load and RMS is relatively strong. For this particular example it is even stronger than for the RPM and RMS.

6 Conclusions

Starting March 17th, 2014, the team has obtained a modified and fixes version of the test bench provided by the manufacturer. The new equipment turned out to work reliable. Undertaken tests have shown inevitable imperfections connected to the TCP/IP protocol performance, which have led to few code modifications.

The next research activities include supplementary data measurements.

For all tasks, vibration signals should be collected in parallel from three measurement channels. Sampling frequency should be between 24 kHz to 50kHz, depends on available data acquisition unit. Time of acquisition of each signal should be 10s unless stated otherwise in detailed description. Used vibration sensors should have smallest possible sensitivity and the best possible magnitude-frequency characteristic. Placement of sensors for both tasks is as follows:

- gearbox - any direction
- test bearing casing - perpendicular to the shaft axis
- one of good bearings casing - perpendicular to the shaft axis (closer to gearbox)

Additionally, raw phase marker signals should be recorded with the same acquisition parameters. Corresponding value of lad should be recorded with highest possible precision and sampling frequency. Detailed description of operational conditions for both measurement tasks is presented below.

Task I. Measurements under varying rotational speed

For three sizes of unbalance (no unbalance, low, high) of the main shaft ten series of the following measurement should be taken.

- Ten (10) seconds length signals. Manually introduced variations of rotational speed from minimal to maximal value. Variations should not be linear but introduced randomly.
- Sixty (60) seconds length signals. Manually introduced variations of rotational speed from

minimal to maximal value. Variations should not be linear but introduced randomly.

For three sizes of bearing faults (no unbalance, low, high) of the main shaft ten series of the following measurement should be taken.

- Ten (10) seconds length signals. Manually introduced variations of rotational speed from minimal to maximal value. Variations should not be linear but introduced randomly.
- Sixty (60) seconds length signals. Manually introduced variations of rotational speed from minimal to maximal value. Variations should not be linear but introduced randomly.

Task II. Examination of the influence of variable operational conditions on discrete signal components

Three different dynamic conditions of the test rig:

- Balanced
- Low unbalance (one bolt)
- High unbalance (three bolts)

No bearing fault.

For each dynamic state of the test rig at least ten measurement series should be collected. Values of load and rotational speed for each series are given in the table 1.

Table 1. Values of rotational speed and load as a percentage of their maximal values. For measurement task I vibration signals should be recorded for each value of rotational speed and load (total 110 measurements).

Speed→ Load ↓	10%	20%	30%	40%	50%	60%	70%	80%	90%	100%
0%	x	x	x	x	x	x	x	x	x	x
10%	x	x	x	x	x	x	x	x	x	x
20%	x	x	x	x	x	x	x	x	x	x
30%	x	x	x	x	x	x	x	x	x	x
40%	x	x	x	x	x	x	x	x	x	x
50%	x	x	x	x	x	x	x	x	x	x
60%	x	x	x	x	x	x	x	x	x	x
70%	x	x	x	x	x	x	x	x	x	x

80%	x	x	x	x	x	x	x	x	x	x
90%	x	x	x	x	x	x	x	x	x	x
100%	x	x	x	x	x	x	x	x	x	x

Task III. Examination of the influence of variable operational conditions on random signal components

Three different dynamic conditions of the test rig:

- No bearing fault
- Small local bearing fault
- Large local bearing fault

Test rig main shaft should be balanced.

For each dynamic state of the test rig at least ten measurement series should be collected. Values of load and rotational speed for each series are given in the table 2.

Table 2. Values of rotational speed and load as a percentage of their maximal values. For measurement task I vibration signals should be recorded for each value of rotational speed and load (total 110 measurements).

Speed→ Load ↓	10%	20%	30%	40%	50%	60%	70%	80%	90%	100%
0%	x	x	x	x	x	x	x	x	x	x
10%	x	x	x	x	x	x	x	x	x	x
20%	x	x	x	x	x	x	x	x	x	x
30%	x	x	x	x	x	x	x	x	x	x
40%	x	x	x	x	x	x	x	x	x	x
50%	x	x	x	x	x	x	x	x	x	x
60%	x	x	x	x	x	x	x	x	x	x
70%	x	x	x	x	x	x	x	x	x	x
80%	x	x	x	x	x	x	x	x	x	x
90%	x	x	x	x	x	x	x	x	x	x
100%	x	x	x	x	x	x	x	x	x	x

7 Bibliography

[1] Bartelmus W, Zimroz R (2009) A new feature for monitoring the condition of gearboxes in non-stationary operation conditions. Mech. Syst. and Signal Proc. 23/5 : 1528-1534

[2] Zimroz, R., Bartelmus, W., Barszcz, T., Urbanek, J., ,Diagnostics of bearings in presence of strong operating conditions non-stationarity—A procedure of load-dependent features processing with application to wind turbine bearings,Mechanical Systems and Signal Processing, 2013,Academic Press"

[3] Urbanek, J., Strączkiewicz, M., Barszcz, T.,; ,Joint Power-Speed Representation of Vibration Features. Application to Wind Turbine Planetary Gearbox,Advances in Condition Monitoring of Machinery in Non-Stationary Operations,,,197-205,2014,Springer Berlin Heidelberg"

[4] Strączkiewicz, M. Urbanek, J. Barszcz, T., Three-dimensional representation of diagnostic features in application to wind turbines, Diagnostyka, 2012 | nr 4(64) | 9-16